ORIGINAL CONTRIBUTION

Live monitoring of small vessels during development and disease using the flt-1 promoter element

Katia Herz · Jan C. Heinemann · Michael Hesse · Annika Ottersbach ·
Caroline Geisen · Christopher J. Fuegemann · Wilhelm Röll ·
Bernd K. Fleischmann · Daniela Wenzel

Abstract Vessel formation is of critical importance for organ function in the normal and diseased state. In particular, the labeling and quantitation of small vessels prove to be technically challenging using current approaches. We have, therefore, established a transgenic embryonic stem (ES) cell line and a transgenic mouse model where the vascular endothelial growth factor receptor VEGFR-1 (flt-1) promoter drives the expression of the live reporter eGFP. Fluorescence microscopy and immunostainings revealed endothelial-specific eGFP labeling of vascular networks. The expression pattern recapitulates that of the endogenous flt-1 gene, because small and large vessels are labeled by eGFP during embryonic development; after birth, the expression becomes more restricted to small vessels. We have explored this in the cardiovascular system more in detail and found that all small vessels and capillaries within the heart are strongly eGFP+. In addition, myocardial injuries have been induced in transgenic mice and prominent vascular remodeling, and an increase in endothelial cell area within the peri-infarct area could be observed underscoring the utility of this mouse model. Thus, the transgenic flt-1/eGFP models are powerful tools to investigate and quantify vascularization in vivo and to probe the effect of different compounds on vessel formation in vitro.

Keywords flt-1 · eGFP · Endothelium · Transgenic mouse · ES cells

K. Herz · J. C. Heinemann · M. Hesse · A. Ottersbach ·
C. Geisen · C. J. Fuegemann · B. K. Fleischmann ·
D. Wenzel (✉)
Institute of Physiology I, University of Bonn,
Sigmund-Freud-Str. 25, 53127 Bonn, Germany
e-mail: dwenzel@uni-bonn.de

W. Röll
Department of Cardiac Surgery,
University of Bonn, Bonn, Germany

Introduction

Vascular endothelial growth factor (VEGF) is a key molecule for vasculo- and angiogenesis, and is predominantly expressed in tissues with developing capillary networks [2]; at the adult stage, VEGF has been found to be increased upon hypoxia [19, 32]. VEGF is a homodimeric glycoprotein and acts mainly via two receptors, VEGF receptor 1 (VEGFR-1 or Fms like tyrosine kinase, flt-1) and VEGF receptor 2 (VEGFR-2, fetal liver kinase, flk-1). While flk-1 has been identified as the receptor inducing a strong tyrosine kinase activity leading to endothelial cell proliferation, migration and enhanced vascular permeability [1, 22], the role of flt-1 has remained more elusive. Flt-1 knockout mice die at E8.5–9.0 due to vascular overgrowth and uncontrolled vascularization [5] indicating that flt-1 plays a critical role as a negative regulator during embryonic development. Similarly, abnormal angiogenesis in the adult has also been linked to flt-1 receptor function and has been proposed to underlie several diseases such as rheumatoid arthritis, atherosclerosis or diabetes [8, 16]; this is also true for tumor and metastasis formation where flt-1 is suspected to play a role [6, 10].

Because of the expression of flt-1 in ischemic tissues undergoing re-vascularization [15, 39] and its involvement

in various pathological states, we reasoned that transgenic in vitro and in vivo models using the flt-1 promoter would be very interesting. Herein we report the generation of stable, transgenic ES cells and mice in which eGFP expression is driven by the flt-1 promoter. Our data reveal persistent flt-1/eGFP expression in small vessels in the in vitro and in vivo systems. In addition, we also demonstrate the utility of the transgenic mouse model to investigate and quantitate vascularization in the heart after myocardial infarction. This may also prove helpful for the analysis of different signaling pathways in response to cardiac injury [12, 23, 38].

Materials and methods

Generation of flt-1/eGFP vector

For the generation of the flt-1/eGFP vector, the 2.2 kb flt-1 promoter [26] was amplified from murine genomic DNA (Promega, Mannheim, Germany) using a nested polymerase chain reaction (PCR) strategy. In the first step, a larger fragment (2.3 kb) containing the flt-1 promoter was amplified (fw: 5′ GGA GAA ACT ATC GAA GGC CAC AGC 3′, rev: 5′ GTC CCC TCC TGC TTC TGC T 3′). This product was applied as template to amplify the 2.2 kb flt-1 promoter using the primers previously reported by Quinn et al. [26] (fw: 5′ GTC AAA TAC CTG TCT GGC TTC 3′, rev: 5′ GTC CCC TCC TGC TTC TGC T 3′). A third PCR step was carried out using the modified second primer pair in order to introduce restriction sites for EcoRI (fw: 5′ TTC GGA ATT CGT CAA ATA CCT GTC TGG CTT C 3′) and SalI (rev: 5′ ATA TGT CGA CGT CCC CTC CTG CTT CTG CT 3′). Finally, the fragment was digested with EcoRI and SalI to obtain sticky ends, and the flt-1 promoter was inserted into the multiple cloning site of the pEGFP-1 plasmid (Clontech Lab. Inc., Saint-Germain-en-Laye, France) via ligation. The flt-1/eGFP vector was applied for electroporation of D3 and G4 ES cells.

Generation of the flt-1/eGFP BAC vector

BAC clones covering the promoter region of the flt-1 gene (RP24 225B5: 187,203 bps and RP23 300K18: 238,695 bps) were obtained from the Children's Hospital Oakland Research Institute (CHORI); BAC DNA was transferred into SW105 E. coli cells by electroporation (can be obtained from NCI-Frederick website http://recombineering.ncifcrf.gov/). An eGFP-pA cDNA was designed to be inserted at the initiation codon in the first exon of the flt-1 gene within the BACs. Therefore, homologous arms were generated by PCR using the pEGFP-1 vector as template. For this end, the following primers were applied: fw: 5′ CGG CCT CGG

AGA GCG CGG GCA CCG GGC CAA CAG GCC GCG TCT TGC TCA CCT GGC CAC AAC CAT GGT GAG 3′, rev: 5′ TGA GAA GCA GAC ACC CGA GCA GCG CGT AAG GCA AGA CCG CGG TGT CCC AGC CCG CGT TTA TGA ACA AAC GAC 3′. Electrocompetent SW105 E. coli cells containing the BACs were electroporated with the targeting cassette, and clones with successful recombination were selected with kanamycin and chloramphenicol. Homologous recombination was verified by PCR with primers spanning the homology region. Then the flt-1/eGFP BAC was used for electroporation in G4 ES cells.

Generation of transgenic ES cell clones (flt-1/eGFP and flt-1/eGFP BAC ES cells)

To generate transgenic ES cell clones, 5×10^6 D3 or G4 ES cells were electroporated with 40 µg of the linearized flt-1/eGFP vector or the circular flt-1/eGFP BAC in PBS with one pulse at 250 V and 500 µF (Bio-Rad Gene Pulser, Munich, Germany) and plated on 10 cm cell culture dishes with feeder cells. After selection with G418 (300 µg/ml for D3 and 165 µg/ml for G4, Invitrogen, Karlsruhe, Germany), resistant colonies were picked and propagated for differentiation.

Cultivation and differentiation of transgenic ES cell clones

Undifferentiated ES cells of the D3 line (ATCC, Wesel, Germany) were cultured on a feeder layer in Dulbecco's modified Eagle medium (DMEM), supplemented with 15% fetal calf serum (FCS), 0.1 mM nonessential amino acids, 50 µg/ml penicillin and streptomycin solution (all from Invitrogen, Karlsruhe, Germany), 0.1 mM β-mercaptoethanol (Sigma Aldrich, Steinheim, Germany), 500 U/ml leukemia inhibitory factor (LIF, Chemicon, Hofheim, Germany) and G418.

ES cells of the G4 line [7] were cultured in Knockout DMEM (Invitrogen, Karlsruhe, Germany) plus the additives mentioned above (G418 165 µg/ml) and 2.0 mM L-glutamine (Invitrogen, Karlsruhe, Germany).

ES cell differentiation was performed using embryoid body (EB) formation via mass culture [11] or hanging drop method [36]. For differentiation, cells were cultivated in Iscove's MEM high-glucose medium (Invitrogen, Karlsruhe, Germany) supplemented with 20% FCS plus additives in the absence of LIF.

After 5 days of differentiation, transgenic EBs were plated on cover slips coated with 0.1% gelatine solution (Sigma Aldrich, Steinheim, Germany). Then, eGFP expression was evaluated on a daily basis. To examine the re-formation of vascular structures, day 5 EBs were digested by collagenase B (Roche, Mannheim, Germany)

and single cells were plated on a Petri dish coated with 0.1% gelatine.

RT-PCR

For RT-PCR, RNA of flt-1/eGFP EBs at differentiation days 0, 3, 6, 9, 12 and 21 were isolated by the acid guanidine thiocyanate-phenol-bromo-chloro-propane (BCP) extraction method. The integrity of RNA extracts was assessed on a 1% MOPS gel and RNA was visualized by ethidium bromide staining. The amount of total RNA was determined by a NanoDrop spectrometer (Peqlab).

First strand complementary DNA (cDNA) was synthesized using the SuperScript III First-Strand Synthesis SuperMix for qRT-PCR (Invitrogen). Reactions containing no template were performed as a negative control. The following primer sequences were used: flt-1: fw: 5′ TGA GCG ATG TGG AAG GAG AC 3′, rev: 5′ ACA GCA ACA CGC CAT AGG AC 3′, eGFP: fw: 5′ CAT GAA GCA GCA CGA CTT CT 3′, rev: 5′ GCG GAT CTT GAA GTT CAC CT 3′, GAPDH: fw: 5′ TGA GCG ATG TGG AAG GAG AC 3′, rev: 5′ ACA GCA ACA CGC CAT AGG AC 3′.

Western blot

Protein of EBs was isolated on differentiation days 0, 3, 6, 9, 12 and 21 using RIPA buffer containing protease inhibitor C (Boehringer Ingelheim, Germany). Then Western blot was performed as previously described [17, 33, 34]. Briefly, the protein concentrations were determined by a Bradford Assay (Bio Rad, Munich, Germany). For SDS-PAGE, proteins were denatured by boiling in 0.8% SDS and 0.5% β-mercaptoethanol (v/v) and the electrophoresis was performed in a 7.5% polyacrylamide gel. Proteins were blotted with a semidry system (Transblot SD, Bio Rad, Germany) on a nitrocellulose membrane (0.45 μm, Whatman, Dassel, Germany) for 45 min at 15 V. The membrane was blocked with 5% BSA in TBST buffer I (20 mM Tris/HCl, 137 mM NaCl, 0.1% Tween 20, pH 7.6) for 1 h at RT. Incubation with β-actin (Sigma-Aldrich, 1:20,000) and eGFP antibody (Living colors A.v. monoclonal antibody (JL-8), Clontech, 1:1,000) was performed over night at 4°C. The secondary antibody, goat-anti-mouse conjugated HRP (Dianova), was used at a dilution of 1:10,000. For detection, an ECL solution (chemiluminescence, GE Healthcare, Munich, Germany) was employed.

Generation of transgenic flt-1/eGFP BAC mice

All mouse experiments complied with procedures approved by the regional and local Animal Care Committees (8.87-50.10.31.08.199). For generation of transgenic mice G4 flt-1/eGFP (BAC), ES cells were screened for normal 40 chromosome karyotype. The transgenic ES cells were aggregated with diploid morula stage CD1 embryos as described previously [21]. Chimeric mice could be identified by coat color and were bred with CD1 mice to examine germline transmission. Offspring was tested for transgene integration by PCR of the tail tips with the following primer pair: fw: 5′ TTC TTC TGA GCG GGA CTC TG 3′, rev: 5′ GTC TAA GCG GTG ATG CCA AC 3′.

Time lapse microscopy of vessel development in ES cell clones

Flt-1/eGFP BAC EBs were plated on culture dishes with glass bottom (Greiner bio GmbH) and cultivated until day 5 + 5. Time lapse microscopy was performed in a temperature (37°C) and CO_2 (5%) controlled chamber with a fluorescent microscope (Axiovert 200 M, Carl Zeiss MicroImaging, Inc.) using the Colibri system (blue LED), a GFP-filter and a 20× objective. Pictures and movies were generated with the Axiovision Rel. 4.8 software (Zeiss). EBs were monitored up to 48 h and pictures taken every 15 min.

Teratoma assay

For teratoma assays, single transgenic flt-1/eGFP ES cells of the D3 line were obtained by trypsin dissociation (Invitrogen, Karlsruhe, Germany). One million cells were injected subcutaneously into the left and right hindlimb of Fox Chase SCID® Beige Mice (Charles River, Sulzfeld, Germany). Tumors were harvested on day 21 after injection; cryosections were generated and immunohistochemistry (see below) or staining with the hematoxylin and eosin (H&E) method was performed. Pictures of H&E stainings were taken on a Zeiss Axiostar plus equipped with an Axiocam MRc 5 camera.

Immunohistochemistry of EBs, teratomas, embryos and organs

Pictures of E9.5 and E14.5 embryos as well as of whole organs were taken with a Leica MZ 16F stereomicroscope. Tissues were fixated with 4% paraformaldehyde (PFA) in phosphate buffered saline (PBS). Thereafter, teratomas, embryos and organs were transferred to 20% sucrose, cryopreserved and then cryosections were generated. For immunohistochemistry, tissues were permeabilized and stained with primary antibodies against VEGF receptor 2 [VEGFR-2, flk-1, (1:100)], PECAM (1:800, both BD Biosciences, Heidelberg, Germany), VE-Cadherin (1:100, CD144, eBiosience, Frankfurt, Germany), CD45 (Ab-6,

1:800, Chemicon), vimentin (1:1,000, Chemicon) or Oct3/4 (1:100, Santa Cruz). As secondary antibodies, Cy3 or Cy5 anti-rat, anti-mouse or anti-chicken (1:400, Dianova, Hamburg, Germany) were applied. Nuclear staining was performed with Hoechst 33342 (BD, Heidelberg, Germany).

Pictures of stained specimen were taken with an inverted fluorescence microscope Axio Imager with ApoTome optical sectioning module (Zeiss, Jena, Germany).

Myocardial infarction of flt-1/eGFP BAC mice

Myocardial infarctions were generated in 10-week-old flt-1/eGFP BAC mice by cryoinjury ($n = 3$) or left coronary artery (LCA) ligation ($n = 6$) as described previously [11, 28]. Mice were killed 3 or 6 days after injury to determine eGFP+ vessels in the infarcted hearts. For quantitation of endothelial cell area after cryoinfarction, 3 transversal sections per heart at a distance of 100 µm each were analyzed. Microscopic pictures of the sections were acquired with the MosaiX function of the Axiovision software (Zeiss). Then, three regions in each section were defined: native heart tissue was identified based on the autofluorescence of cardiomyocytes, the peri-infarct zone comprised the lesioned and vascularized area without cardiomyocytes, and in the infarct zone only a few single nuclei were found. The eGFP+ area within these regions was measured and normalized to the total area of the respective region.

Statistical analysis

Data are expressed as mean ± SEM. Statistical significance was determined by Student's unpaired t test. $P < 0.05$ was considered statistically significant.

Results

Generation of flt-1/eGFP embryonic stem (ES) cells

To generate flt-1/eGFP ES cells, we first used the 2.2 kb flt-1 promoter element [26] that was isolated from mouse DNA by a nested PCR strategy and cloned into an eGFP plasmid. The vector was used for electroporation of murine ES cells of the D3 and G4 line. Screening revealed that only one out of 18 (D3) and one out of 76 (G4) clones showed eGFP expression restricted to vascular networks. These clones displayed only weak eGFP expression in the undifferentiated state (day 0, Fig. 1a) as has been reported for other endothelial markers such as PECAM [27] or flk-1 [9]. During mesodermal differentiation in the EB system at early stages, we could detect eGFP+ clusters, later bright

Fig. 1 Endothelial-specific eGFP expression in embryoid bodies ▶ (EBs) derived from flt-1/eGFP ES cells. **a–c** Starting from undifferentiated ES cells eGFP+ sprouts (*arrows*) developed in suspension culture of the EB model. **d–f** From these sprouts (*arrow*) vascular networks emerged (*arrow heads*) which could be best visualized during adherent growth after plating of the EBs on day 5. **g–n** Immunostaining of EBs showed that eGFP+ (*green*) vascular structures co-localized with flk-1+ (*red*, **g, h, j**) and PECAM+ (**k, l, n**) endothelial cells, *blue* = Hoechst, *bars* 300 µm (**a–f**), 200 µm (**g, k**), 100 µm (**h–j, l–n**). **o** Time course of flt-1 and eGFP mRNA expression levels revealed peak signals on day 9. **p** Time course of eGFP protein expression yielded peak levels on day 12

eGFP+ elongated branches (Fig. 1b–d, arrows) developed giving origin to extensive eGFP+ networks that can be best seen after plating (Fig. 1d–f, arrow heads). Immunohistochemistry of EBs revealed that flt-1/eGFP and the endothelial specific marker flk-1 were to some degree differentially expressed in cell clusters of very early differentiation stage EBs, whereas there was almost a complete overlap between eGFP expression (green) and staining for the endothelial cell markers flk-1 (red, Fig. 1g, h, j) and PECAM (red, Fig. 1k, l, n) in endothelial tubes at later stages. We determined the endothelial specificity of the flt-1-driven eGFP expression more in detail by analyzing the overlap between eGFP fluorescence and PECAM immunostaining at the single cell level (approximately 1,000 cells) upon dissociation of EBs 5 days after plating (day 5 + 5 EBs). We found that 92.7% of the cells were eGFP+ PECAM+, 6.4% eGFP− PECAM+ and only 0.9% eGFP+ PECAM−. Thus, on day 10 of differentiation, almost all PECAM+ cells showed eGFP fluorescence, while only very few cells were eGFP+ but PECAM−. We tried to further characterize the cell biological identity of this subtype and found that some of these eGFP+ PECAM− cells displayed weak Oct3/4 staining (data not shown) suggesting that these were, as reported earlier [18], undifferentiated flt-1 expressing ES cells; other cells were stained by an antibody against vimentin, indicating mesodermal identity. We next explored the eGFP labeling in newly forming vessels; for this purpose, day 5 EBs were dissociated into single cells. Within 3 days after re-plating, sprouting of eGFP+ cells appeared and within 7 days even prominent vascular network formation could be detected (Suppl. Fig. 1a–d). The kinetics of flt-1 and eGFP expression was also evaluated by PCR and revealed that flt-1 mRNA expression was very low until day 3 of differentiation and peaked on day 9, similar as the eGFP mRNA expression (Fig. 1o). These kinetics were corroborated by Western blot analysis of eGFP protein expression; here, peak levels were measured on day 12 (Fig. 1p). Thus, the 2.2 kb flt-1 promoter element driving eGFP generated an endothelial-specific expression pattern in differentiating ES cells with a peak expression around days 9–12. However, with the 2.2 kb flt-1 promoter element, only very few
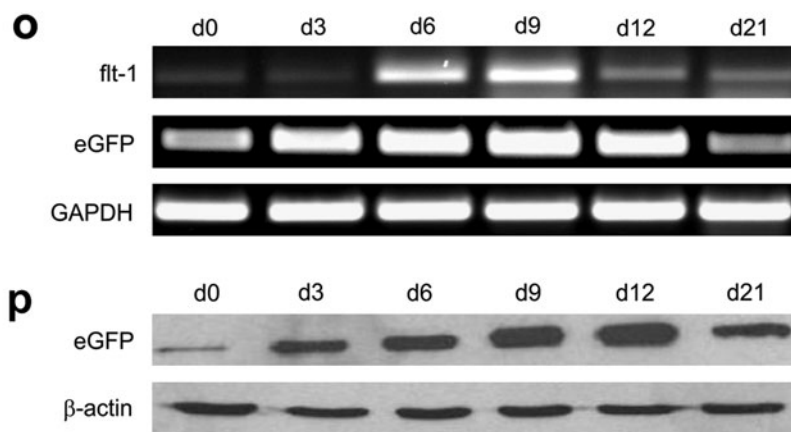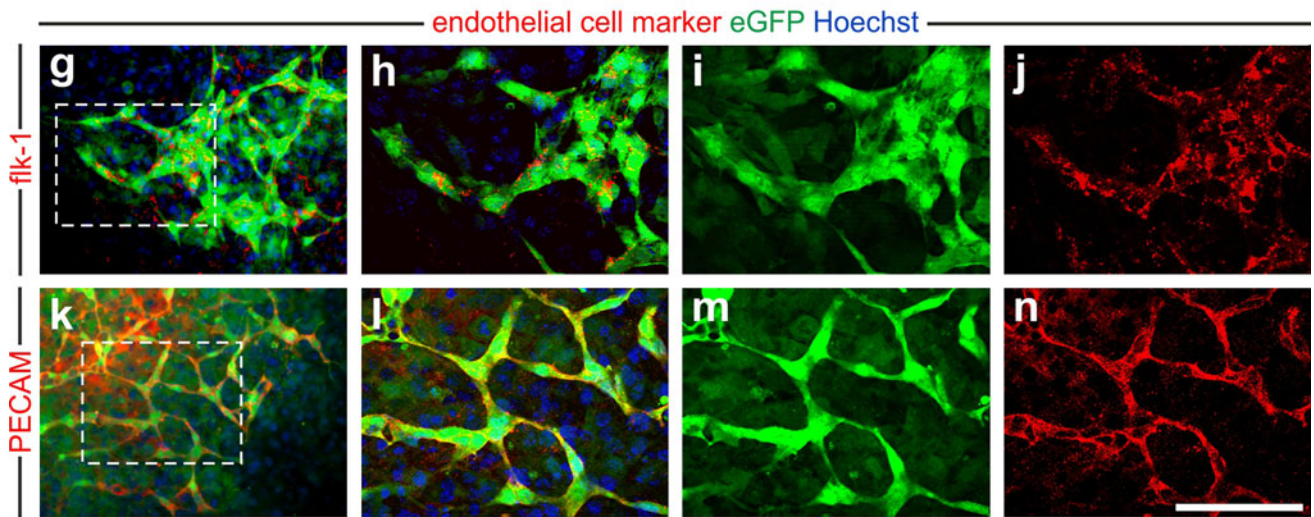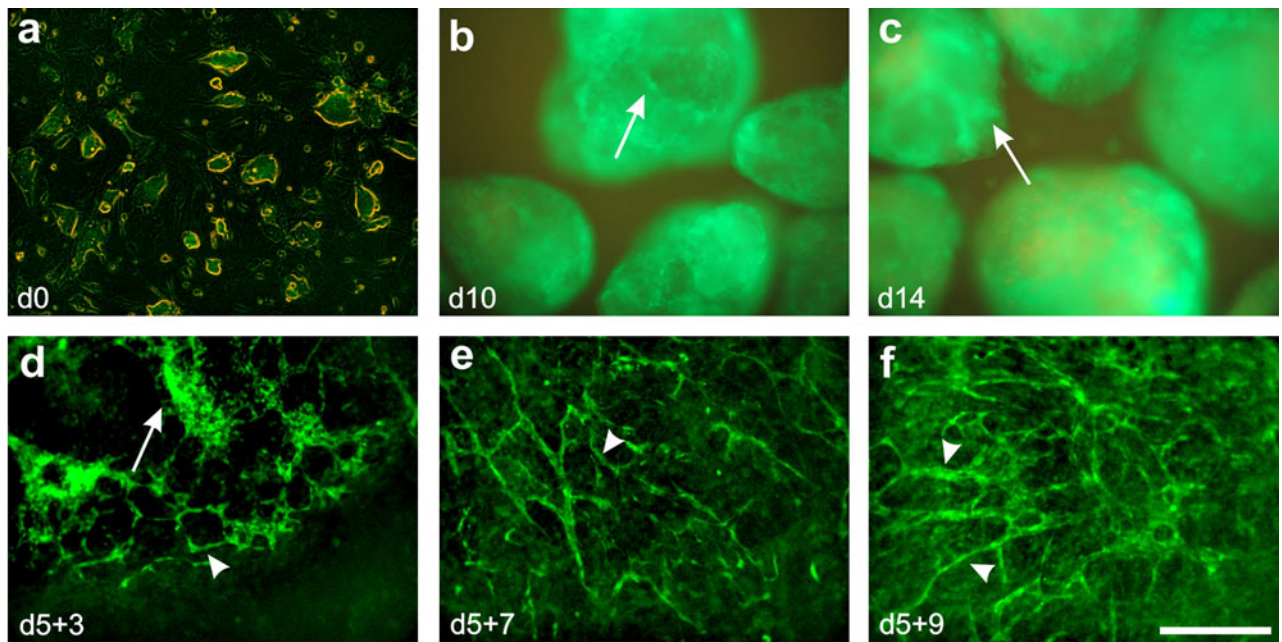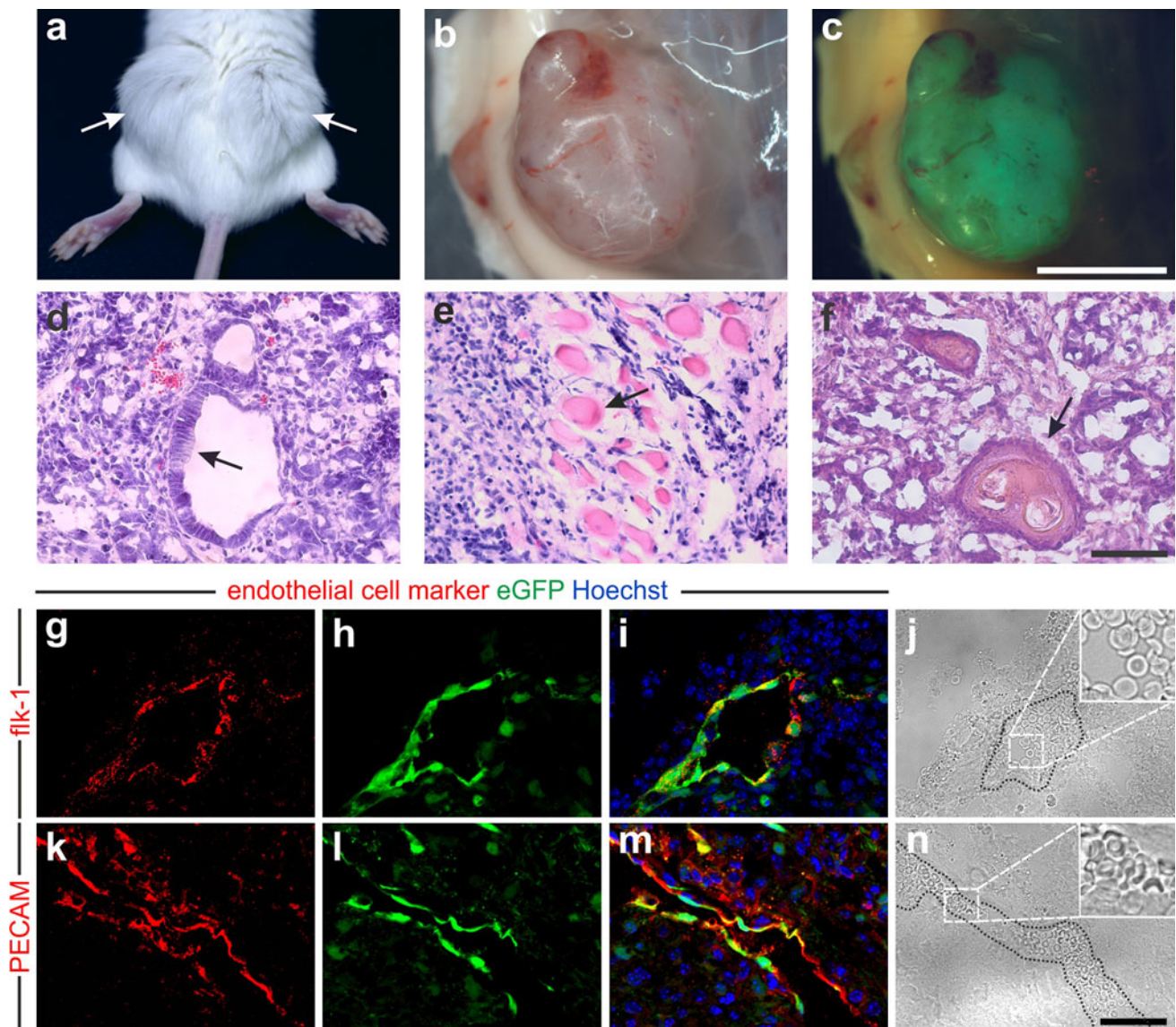
Fig. 2 EGFP+ vascular structures in flt-1/eGFP ES cell-derived teratomas in SCID mice. **a–c** Teratomas in hindlimb of mice displayed eGFP+ areas under fluorescence light (**c**). In the teratomas tissue types of the three germ layers were found: columnar epithelium (endoderm, *arrow*, **d**), muscle cells (mesoderm, *arrow*, **e**) and squamous epithelium (ectoderm, *arrow*, **f**). Sections revealed overlap between eGFP (*green*, **h**, **i**, **l**, **m**) with flk-1 (*red*, **g**, **i**) and PECAM (*red*, **k**, **m**) immunostainings. Bright field pictures showed that vascular structures contained erythrocytes (*insets*) in their lumina (**j**, **n**), *blue* = Hoechst, *bars* 500 μm (**a–c**), 200 μm (**d–f**), 100 μm (**g–n**), 25 μm (*insets*)

transgenic ES cell clones with endothelial-specific eGFP labeling could be obtained.

Flt-1/eGFP ES cells can generate eGFP+ vessels in vivo

Next, we wanted to explore whether the flt-1/eGFP ES cells could yield vascular structures in vivo, and to this end flt-1/eGFP ES cells were injected subcutaneously into severely combined immune-deficient (SCID) mice. 3 weeks after injection, teratoma-like tumor masses had formed (Fig. 2a, b),

which displayed prominent eGFP fluorescence signals under the stereomicroscope (Fig. 2c). Teratoma formation was confirmed by histological analysis, because derivatives of all three germ layers such as columnar epithelium (endoderm, Fig. 2d, arrow), muscle (mesoderm, Fig. 2e, arrow) and squamous epithelium (ectoderm, Fig. 2f, arrow) could be found. Fluorescence microscopy of cryosections revealed high numbers of eGFP+ cells (Fig. 2h, i, l, m); their endothelial nature was confirmed by immunostainings for flk-1 (Fig. 2g, i) and PECAM (Fig. 2k, m). We further investigated eGFP+ vascular structures using bright field

microscopy (Fig. 2j, n) and found that these were likely functional blood vessels due to their content of red blood cells (Fig. 2j, n, insets). These experiments show that flt-1/eGFP ES cells can build up vessels in vivo.

Because of the endothelial-specific eGFP expression in vitro and in vivo, we wanted to generate a transgenic mouse model in order to enable the identification of blood vessels in different organs in vivo. One possibility is the diploid or tetraploid aggregation of ES cells with wild-type mouse embryos which yields a mouse with an identical genetic background as in the in vitro system. However, when performing karyotyping of the two ES cell clones, we found a high percentage of cells with chromosomal aberrations in both cases. In fact, aggregation of those transgenic ES cells with diploid morula stage CD1 embryos only produced two animals with a high degree of chimerism but no germ-line transmission. We also tested direct generation of transgenic mice by pronuclear injection of the construct, but the 33 transgenic animals obtained by this method displayed unspecific expression outside the vascular system (data not shown).

Generation of flt-1/eGFP BAC ES cells

As the 2.2 kb flt-1 promoter element produced only two clones with endothelial-specific reporter gene expression and no transgenic mice with the expected expression pattern, we suspected that the promoter may be subject to negative position effects or that critical regulatory elements of the flt-1 promoter may be missing. We, therefore, chose the bacterial artificial chromosome (BAC) technology for the generation of new transgenic ES cell lines. EGFP-pA cDNA was inserted into the first exon of two different BACs spanning the murine flt-1 promoter region by homologous recombination (Fig. 3a). The resulting flt-1/eGFP BAC constructs were used for electroporation of G4 ES cells [7]. G418 selection provided nine clones and four of these displayed a uniform expression pattern with obvious endothelial-specific eGFP labeling during differentiation. The time-course of eGFP expression and network formation proved to be very similar to the above-described flt-1/eGFP clones with weak eGFP expression at the undifferentiated stage, first vascular structures around day 7 and a peak of vascular network formation around day 12 of differentiation. The vascular networks covered large areas of the EBs and were clearly visible up to late stages of differentiation (day 5 + 13, Fig. 3b); their formation via sprouting angiogenesis could be monitored with time lapse microscopy (Suppl. Video 1). In analogy to the flt-1/eGFP clones, immunohistochemistry revealed almost a complete overlap of the eGFP expression with staining for flk-1 (Fig. 3c–e), PECAM (Fig. 3f–h) and also VE-Cadherin (Fig. 3i–k) on day 5 + 6. These experimental results

demonstrated that transfection of ES cells with the flt-1/eGFP BAC construct provides clones with endothelial-specific eGFP expression at a very high frequency.

Generation of flt-1/eGFP BAC transgenic mice

For the generation of transgenic mice, flt-1/eGFP BAC ES cell clones were karyotyped and diploid aggregation with CD1 embryos was performed. Eight chimeric mice with a high degree of coat color chimerism were obtained. Seven of them provided germ-line transmission when bred with CD1 mice. Flt-1/eGFP BAC mice were viable and fertile and no obvious adverse side effects of the flt1/eGFP expression on development and growth were noted.

Main focus of our analysis of the mice was the expression pattern in the cardiovascular system due to our scientific interest in its development and diseased state. First, we investigated the eGFP expression under fluorescence light at an early (E9.5) and a later (E14.5) embryonic developmental stage. Flt-1/eGFP BAC embryos at E9.5 were transparent and displayed bright eGFP expression in large and small vessels (Fig. 4a–c). PECAM-stained slices evidenced a very good overlap with eGFP fluorescence (Fig. 4d); especially, the endocardium of the heart and the outflow tract were strongly labeled by eGFP (Fig. 4e, f). At E14.5, an almost homogeneous fluorescence was observed caused by the vascularized skin (Fig. 4g). The strong eGFP labeling of large and small vessels was also seen at this stage (Fig. 4h). In the heart, in particular, the valves were highly fluorescent (Fig. 4i, j). Next, we characterized the mice at the adult stage; the transgenic mice could be identified by their eGFP fluorescence in the ears using a trans-illumination approach. When whole organs were analyzed with a stereomicroscope, the eGFP fluorescence was found in vascular structures of all organs except the liver, namely the eye (Fig. 5a), the brain (Fig. 5b) and the skin (Fig. 5c). Immunohistochemistry of cryosections with PECAM antibody (red) evidenced that the native eGFP (green) expression was restricted to the vascular endothelium in the organs analyzed, such as the intestinal villi of the gut (Fig. 5d–f), the lung (Fig. 5g–i), the thymus (Suppl. Fig. 2a–c) and the kidney (Suppl. Fig. 2d–f) with vasa recta and glomeruli (inset). Within the heart, we investigated the eGFP expression in detail and found that all small vessels with a diameter below 50 μm displayed strong eGFP expression and a complete overlap with PECAM staining, while larger vessels were eGFP− (Fig. 5j–l, inset). EGFP expression was endothelial-specific as smooth muscle cells and cardiomyocytes were eGFP− (Fig. 5j–l). Interestingly, the endothelium in large arteries such as aorta (Suppl. Fig. 3a–c) or carotid artery (Suppl. Fig. 3d–f) was entirely eGFP−, whereas that of larger veins such as
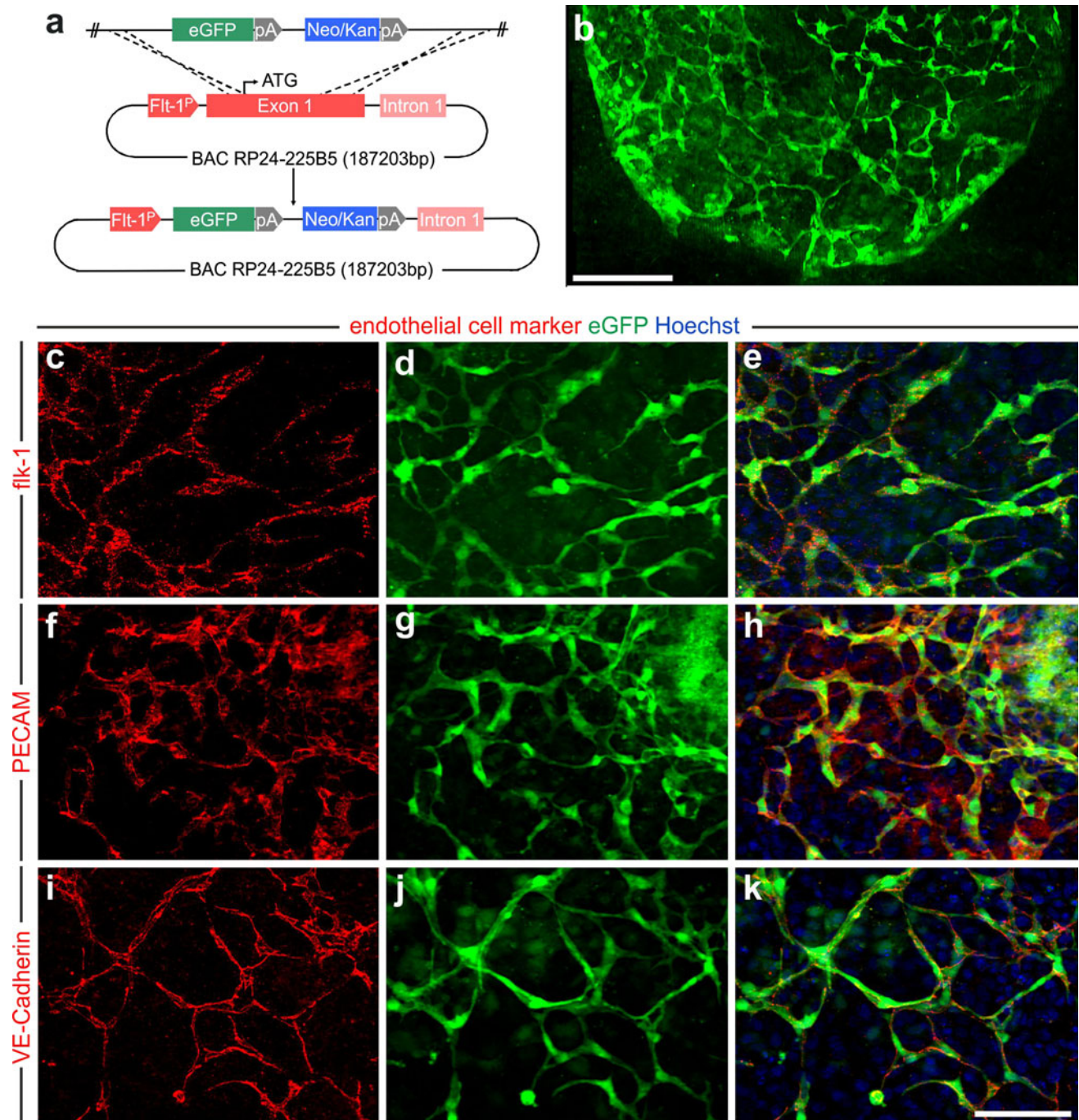
Fig. 3 Endothelial-specific eGFP expression in embryoid bodies (EBs) derived from flt-1/eGFP BAC ES cells. **a** Scheme of BAC recombination strategy. **b** Overview of a highly vascularized EB on day 5+13 (green = eGFP). **c–j** Immunostainings of eGFP+ (green) vascular networks proved their endothelial origin [red = flk-1 (**c**, **e**), PECAM (**f**, **h**), VE-Cadherin (**i**, **k**), blue = Hoechst], bars 200 μm (**b**), 100 μm (**c–k**)

the jugular vein was strongly labeled (Suppl. Fig. 3g–i). Thus, the flt-1/eGFP BAC mouse line is a valid tool to determine flt-1 expression during development and to visualize small vessels in a variety of different organs at the adult stage; prominent eGFP expression was found in all endothelial cells of small vessels in the adult heart.

Vascularization of myocardial infarction in flt-1/eGFP BAC mice

Because of the excellent eGFP labeling of small vessels in the flt-1/eGFP BAC mice, we hypothesized that this model enables characterization and quantitation of the
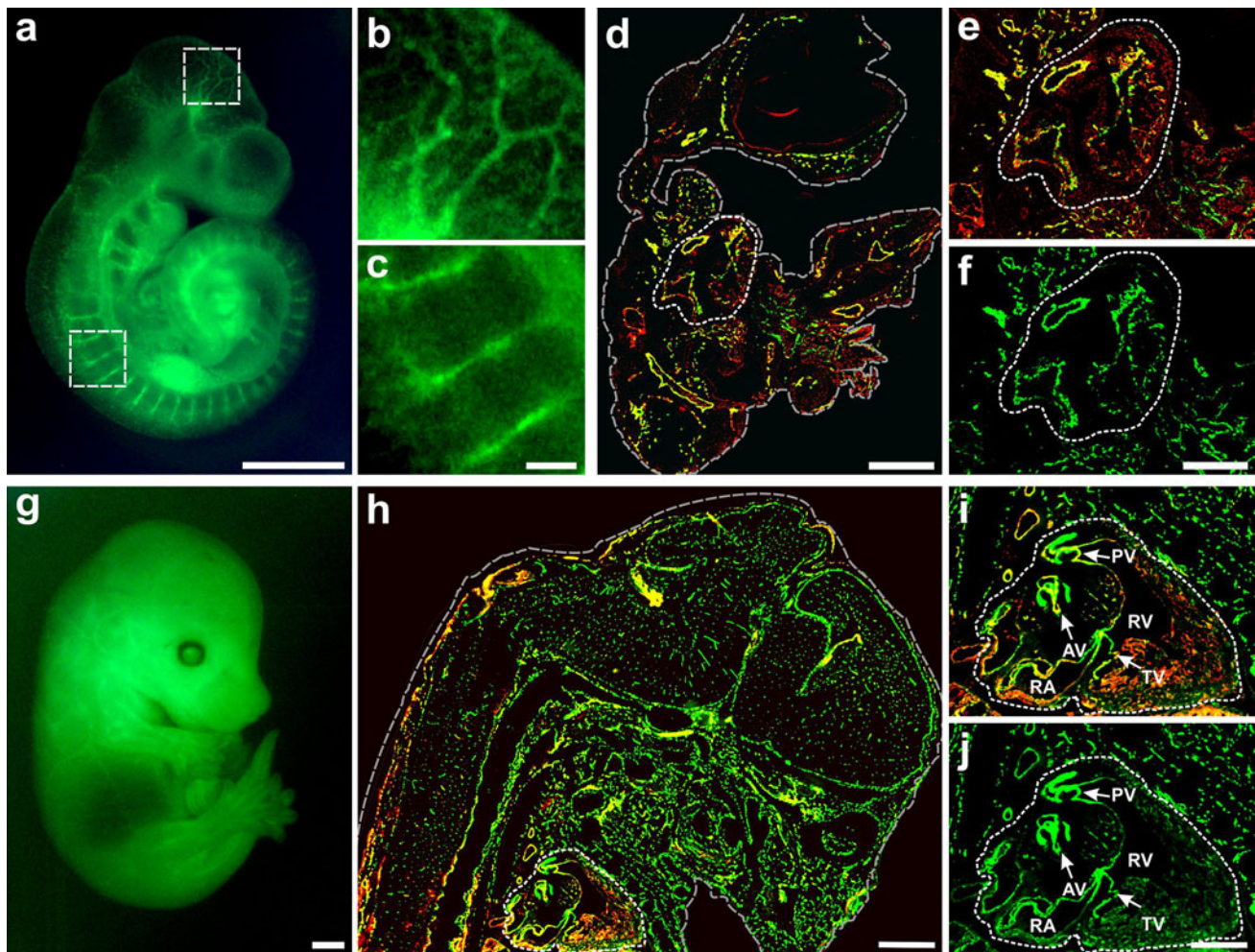
Fig. 4 EGFP expression in flt-1/eGFP BAC embryos. **a–c** Fluorescence pictures revealed that heterozygous flt-1/eGFP embryos at E9.5 were highly transparent; large and small vessels proved strongly eGFP+; distinct eGFP+ vessels could be found at the head (**b**) and in the intersomitic region (**c**), the *dotted squares* define the regions of the embryo with magnifications in **b** and **c**. **d** In sections of E9.5 embryos a high overlap of eGFP (*green*) with PECAM staining (*red*) was observed. **e, f** In the heart of E9.5 embryos strong eGFP (*green*) and PECAM (*red*) expression was seen in the endocardium of the cavities and the outflow tract. **g** At E14.5 eGFP+ vessels in the skin produced a bright eGFP signal throughout the body. **h** Sections of E14.5 embryos showed flt-1/eGFP (*green*) expression in large and small arteries (PECAM = *red*). **i, j** At this stage the heart valves displayed a very strong eGFP (*green*) signal (*RA* right atrium, *RV* right ventricle, *PV* pulmonary valve, *AV* aortic valve, *TV* tricuspidal valve, PECAM = *red*). Note that the *dotted grey lines* label the surface of the embryo (**d, h**) and the *dotted white lines* define the embryonic heart (**d–f, h–j**). *Bars* 1,000 μm (**a, g**), 125 μm (**b, c**), 500 μm (**d, h**), 250 μm (**e, f**), 200 mm (**i, j**)

vascularization in organs post-injury. After myocardial infarction, the vascularization of the infarct and peri-infarct areas are critical determinants of survival and remodeling in the heart; we, therefore, assessed the utility of our flt-1/eGFP BAC transgenic mouse in infarct models. This type of analysis is currently strongly limited using standard immunohistochemistry due to problems with antibody staining or strong background signals in the infarct regions. We induced cryoinjury or left coronary artery ligation and investigated the ensuing re-vascularization. The cryoinjury has the distinct advantage of reproducible lesions, uniform tissue necrosis of the injured area within the first 3 days and fibrotic repair in the following few days [29]. 3 and

6 days after the procedure, the lesion site could be easily identified in flt-1/eGFP BAC mice using macroscopic bright field and fluorescence pictures (Fig. 6a–d). On day 3 after cryoinfarction there were, as expected, almost no intact cells and no eGFP fluorescence found in the center of the lesion (Fig. 6e). In contrast, in the peri-infarct area, a high number of eGFP+ round-shaped structures displaying distinct lumen formation could be detected (Fig. 6f), whereas native cardiomyocytes and capillaries without obvious lumina were found in the non-infarcted border zone (Fig. 6g). The vascular eGFP+ structures in the peri-infarct zone (Fig. 6h) were clearly endothelial cells due to positive PECAM staining (Fig. 6i, j) and negative staining
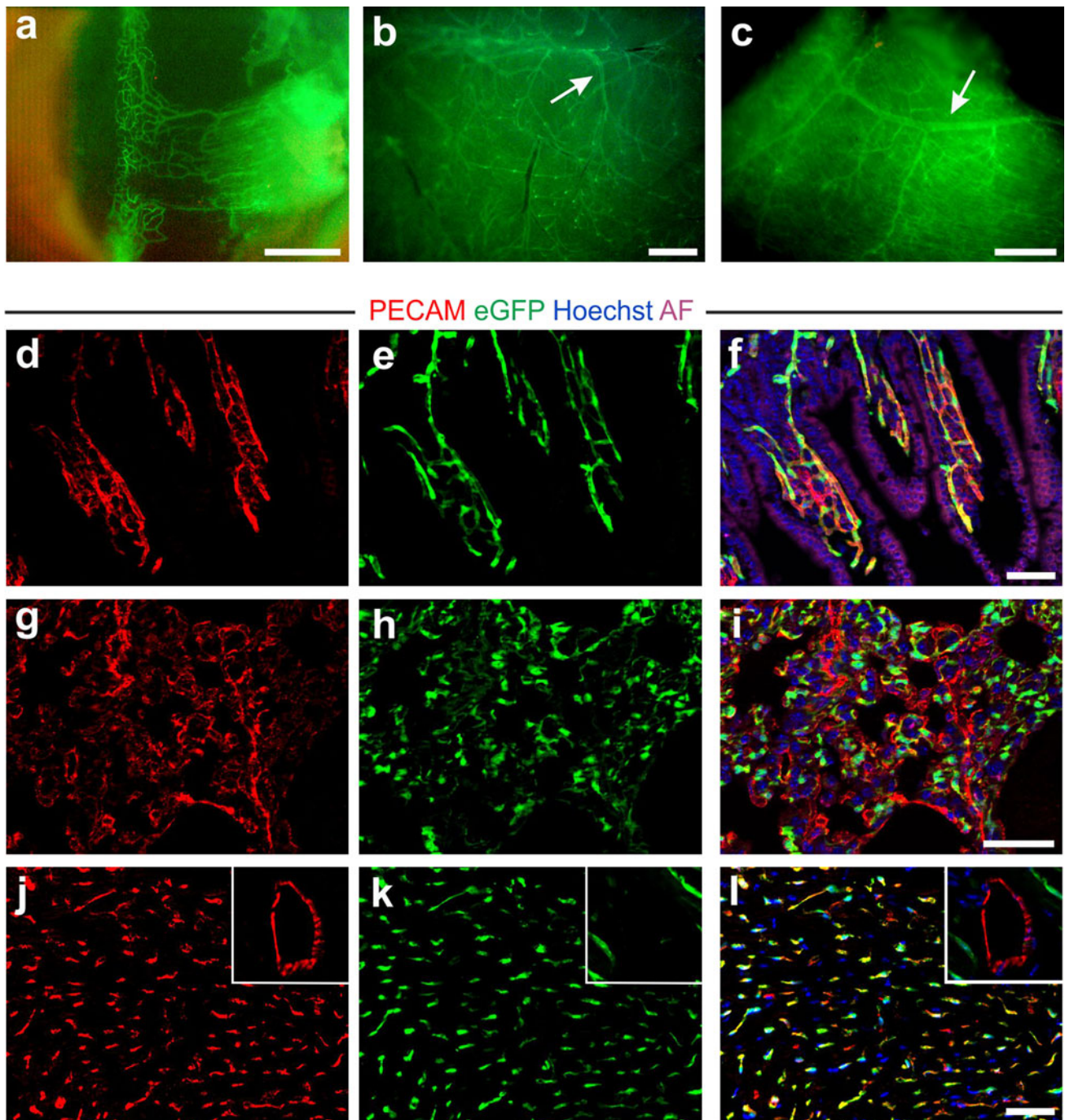
Fig. 5 EGFP expression pattern in adult organs of flt-1/eGFP BAC mice. Flt-1/eGFP BAC chimeric mice showed prominent eGFP (*green*) expression in vessels of the eye (**a**), the brain (**b**) and the skin (**c**). Immunostainings demonstrated bright eGFP+ capillaries in intestinal villi of the gut (**d–f**) and the lung (**g–i**) of chimeric and in the heart of heterozygous mice (**j–l**), *inset*: larger vessels were eGFP− but PECAM+ (*red* = PECAM, *blue* = Hoechst, *magenta* = autofluorescence). *Bars* 200 μm (**a–c**), 50 μm (**d–l**), 75 μm (*inset*)

against the pan-hematopoietic marker CD45 (Suppl. Fig. 4); interestingly, at this stage, the PECAM staining was relatively weak. On day 6 after cryoinfarction, a few small vessels could be found in the central part of the lesion, most probably because of re-vascularization (Fig. 6k, arrow). The eGFP+ endothelial cells in the peri-

infarct zone had formed into more straight and elongated structures indicating pronounced vascular remodeling (Fig. 6l), whereas the vascular structures in the non-infarcted regions remained unaltered (Fig. 6m). The vascular structures in the peri-infarct zone at this stage displayed stronger eGFP and PECAM expression compared to

day 3 (Fig. 6n–p), possibly indicating a more mature stage. When the relative area of eGFP+ cells in the peri-infarct zone was measured, we found a strong increase after 6 days (0.027 ± 0.001, $n = 6$) compared to 3 days (0.016 ± 0.001, $n = 3$); in contrast, there was no detectable change in the endothelial area of the native myocardium (Fig. 6q). We also applied left coronary artery (LCA) ligations in the flt-1/eGFP BAC mouse which is a more physiological injury model; the infarct areas were less regular and well-defined compared to cryoinjuries and therefore quantitation of re-vascularization was not performed. At 3 days after the occlusion, there were infarct zones with almost no eGFP+ vascular structures (Fig. 6r), but in the peri-infarct areas small sinuous eGFP+ vessels were detected (Fig. 6s). At 6 days after occlusion, eGFP+ structures were found within the infarct (Fig. 6u), whereas eGFP+ elongated vessels were visible in the peri-infarct zone, some of these with lumen formation (Fig. 6v, arrow). The heart structure in the non-infarcted areas was, as expected, unperturbed (Fig. 6t, w). Thus, the overall morphological characteristics of the vascular remodeling proved very similar in both myocardial lesion models.

Our data demonstrate that the flt-1/eGFP BAC mouse allows direct visualization of small vessels in the heart, and therefore facilitates the analysis of vascularization upon different types of myocardial injury.

Discussion

Aim of the present study was to generate novel transgenic in vitro and in vivo models in which small vessels are labeled by a fluorescent reporter molecule. We have chosen the flt-1 promoter because it has been proposed as a bona fide marker of endothelial cells in general and, in particular, of small vessels. Furthermore, this promoter has also attracted our attention due to its reported up-regulation and involvement in re-vasulization of the ischemic heart [13, 15]. However, to date, the flt-1 expression pattern could be only characterized with molecular approaches and with the help of a lacZ knock in mouse model due to the lack of specific antibodies. Our experimental data prove that the flt-1 driven eGFP expression is endothelial cell-specific in the vasculature, strongly labels small vessels in various organs and provides an excellent approach to monitor vascularization during development and disease.

We found that BAC constructs strongly increased the efficiency of generating transgenic ES cell lines with an endothelial-specific expression pattern compared to the use of shorter promoter segments. This points to the relevance of negative position effects or additional regulatory sequences outside of the 2.2 kb flt-1 promoter element that most likely determine tissue specificity. We noticed weak

flt-1 mRNA expression in undifferentiated flt-1/eGFP ES cell lines which is in line with other studies, where low mRNA levels of the VEGF receptors flt-1 [18] and flk-1 [9] were reported in undifferentiated ES cells. Even though flt-1 and eGFP mRNA expression were both driven by the flt-1 promoter, we found high eGFP mRNA and protein levels at this stage. Because this is the case for the 2.2 kb promoter element as well as for the BAC, it is unlikely due to the lack of regulatory sequences, but suggests that either eGFP mRNA processing is more efficient or eGFP mRNA is more stable compared to flt-1 mRNA [30].

During ES cell differentiation and starting from relatively early embryonic developmental stages in mouse, endothelial-specific eGFP expression in the vasculature was detected. In fact, in the transgenic mouse eGFP+ vessels were found at all developmental stages from the embryo to the adult. However, obvious differences in the expression pattern were noticed. At the embryonic stage both large and small vessels were eGFP+; furthermore, the cardiac valves were strongly positive which fits to the reported relevance of flt-1 as a regulator of VEGF signals for endothelial to mesenchymal transition in the outflow tract [31] or in the atrioventricular canal [4] during heart valve formation. Overall, the embryonic expression pattern of flt-1/eGFP overlapped with earlier studies using in situ hybridization or lacZ staining [2, 5]. While flt-1 expression was thought to primarily label developing endothelium, our experimental data demonstrate that it is strongly expressed in all small vessels also at the adult stage. This finding supports the assumption that flt-1 also labels quiescent endothelium [25, 35]. In contrast to the embryo, there was no eGFP signal in large arteries, whereas the endothelium of large veins was labeled. Small arteries are thought to play a critical role for vascular remodeling and re-vascularization in response to intermittent or permanent ischemia in the heart and we therefore probed this hypothesis by inducing different types of cardiac lesions in our transgenic mice. We found large clusters of eGFP+ endothelial cells in the peri-infarct area on day 3 post-lesion. The elongation of these structures between day 3 and 6 as well as the concomitant increase of eGFP and PECAM expression could be indicative for the maturation of these vascular structures. In addition, in the center of the lesion no eGFP+ vessels were visible on day 3 after cryoinjury. Between day 3 and 6, small vascular structures were found to emerge indicating re-vascularization. Similar morphological changes were also found when analyzing re-vascularization at different time points after LCA ligation.

Thus, the endothelial cell-specific eGFP labeling in ES cells and transgenic mice enables to visualize vascularization in early developmental stages and upon injury; moreover by these transgenic models, the screening of drugs and compounds for embryotoxic effects and/or their
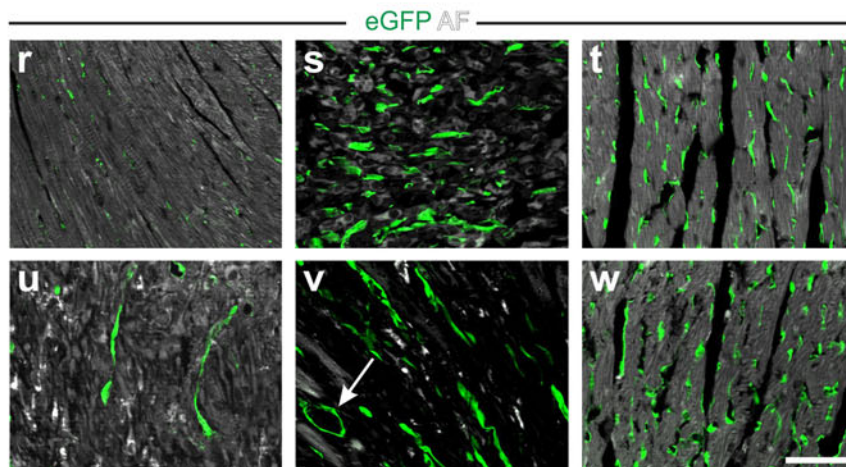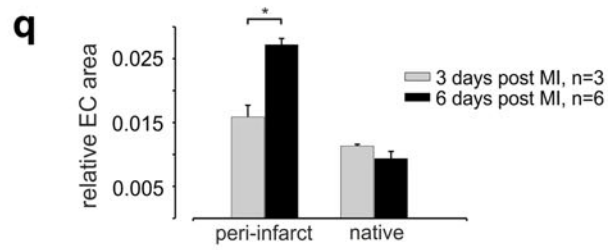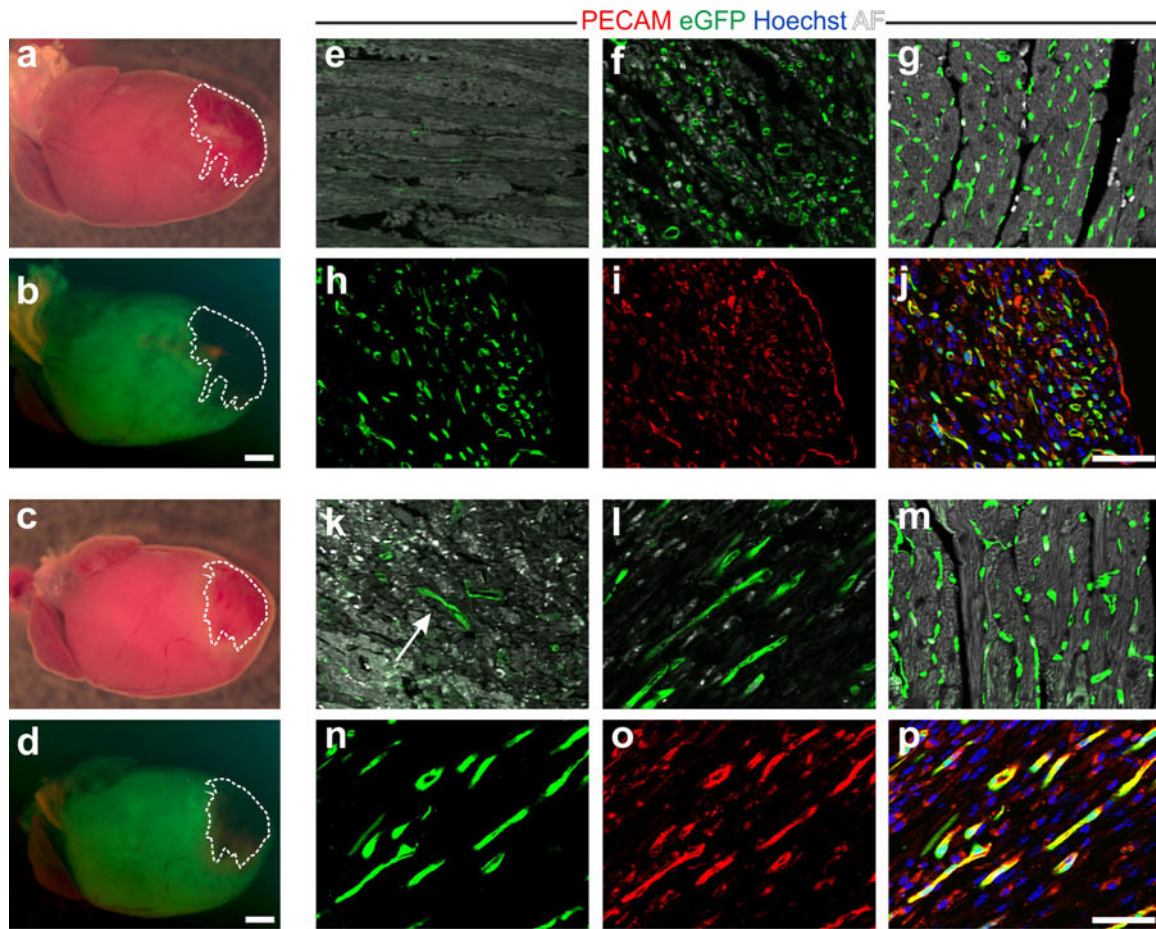
◀ **Fig. 6** Myocardial injury in flt-1/eGFP BAC mice. Bright field and fluorescence stereomicroscopic pictures of heterozygous mouse hearts 3 (**a**, **b**) and 6 (**c**, **d**) days after cryoinfarction, the lesions are marked by the dotted lines. Representative pictures of vascularization 3 days after cryoinfarction: there were no vessels in the infarcted area (**e**), round-shaped eGFP+ vascular structures with lumina were seen in the peri-infarct zone (**f**) and a normal distribution of capillaries was noticed in native myocardium (**g**) (*green* = eGFP, *white* = autofluorescence). **h–j** Immunostaining of a cryosection of the peri-infarct zone (day 3) showed a high number of eGFP+ small capillaries (*green* = eGFP, *red* = PECAM, *blue* = Hoechst). Representative pictures of vascularization 6 days after cryoinfarction: single eGFP+ capillaries (*arrow*) were found in the infarct area (**k**), larger elongated eGFP+ vessels in the peri-infarct zone (**l**) and a normal distribution of capillaries was observed in native myocardium (**m**) (*green* = eGFP, *white* = autofluorescence). **n–p** Immunostaining of a cryosection of the peri-infarct zone yielded a high number of larger longitudinally cut eGFP+ PECAM+ capillaries; note the higher intensity of eGFP and PECAM signals compared to day 3 (*green* = eGFP, *red* = PE-CAM, *blue* = Hoechst). **q** Statistical analysis of relative eGFP+ endothelial cell (EC) area in the peri-infarct zone and native myocardium 3 and 6 days after cryoinfarction (MI). Representative pictures of vascularization 3 days after LCA ligation: almost no vessels were found in the infarcted area (**r**), eGFP+ vascular structures with a sinuous shape were seen in the peri-infarct zone (**s**) and a normal distribution of capillaries was noticed in native myocardium (**t**). Representative pictures of vascularization 6 days after LCA ligation: single eGFP+ capillaries were found in the infarct area (**u**), elongated eGFP+ vessels some with lumen formation (*arrow*) in the peri-infarct zone (**v**) and a normal distribution of capillaries was observed in native myocardium (**w**) (*green* = eGFP, *white* = autofluorescence). *Bars* 1,250 µm (**a–d**), 50 µm (**e–p**, **r–w**)

modulation of vascular structures in vitro and in vivo is possible [3, 14, 20, 24]. In addition, eGFP+ endothelial cells can be highly enriched by fluorescence-activated cell sorting and this allows to determine their molecular and cell biological characteristics as well as their regenerative potential [37]. The experimental data using cardiac injury models suggest that this transgenic mouse model will also be very helpful to further explore mechanisms underlying vascular remodeling and re-vascularization.

References

1. Bernatchez PN, Soker S, Sirois MG (1999) Vascular endothelial growth factor effect on endothelial cell proliferation, migration, and platelet-activating factor synthesis is flk-1-dependent. J Biol Chem 274:31047–31054. doi:10.1074/jbc.274.43.31047

2. Breier G, Clauss M, Risau W (1995) Coordinate expression of vascular endothelial growth factor receptor-1 (flt-1) and its ligand suggests a paracrine regulation of murine vascular development. Dev Dyn 204:228–239. doi:10.1002/aja.1002040303

3. Bremer S, Worth AP, Paparella M, Bigot K, Kolossov E, Fleischmann BK, Hescheler J, Balls M (2001) Establishment of an in vitro reporter gene assay for developmental cardiac toxicity. Toxicol In Vitro 15:215–223. doi:10.1016/S0887-2333(01)00007-8

4. Dor Y, Camenisch TD, Itin A, Fishman GI, McDonald JA, Carmeliet P, Keshet E (2001) A novel role for VEGF in endocardial cushion formation and its potential contribution to congenital heart defects. Development 128:1531–1538

5. Fong GH, Klingensmith J, Wood CR, Rossant J, Breitman ML (1996) Regulation of flt-1 expression during mouse embryogenesis suggests a role in the establishment of vascular endothelium. Dev Dyn 207:1–10. doi:10.1002/(SICI)1097-0177(199609)207:1<1:AID-AJA1>3.0.CO;2-M

6. Frank NY, Schatton T, Kim S, Zhan Q, Wilson BJ, Ma J, Saab KR, Osherov V, Widlund HR, Gasser M, Waaga-Gasser AM, Kupper TS, Murphy GF, Frank MH (2011) VEGFR-1 expressed by malignant melanoma-initiating cells is required for tumor growth. Cancer Res 71:1474–1485

7. George SH, Gertsenstein M, Vintersten K, Korets-Smith E, Murphy J, Stevens ME, Haigh JJ, Nagy A (2007) Developmental and adult phenotyping directly from mutant embryonic stem cells. Proc Natl Acad Sci U S A 104:4455–4460. doi:10.1073/pnas.0609277104

8. Hazarika S, Dokun AO, Li Y, Popel AS, Kontos CD, Annex BH (2007) Impaired angiogenesis after hindlimb ischemia in type 2 diabetes mellitus: differential regulation of vascular endothelial growth factor receptor 1 and soluble vascular endothelial growth factor receptor 1. Circ Res 101:948–956. doi:10.1161/CIRCRESAHA.107.160630

9. Hidaka M, Stanford WL, Bernstein A (1999) Conditional requirement for the flk-1 receptor in the in vitro generation of early hematopoietic cells. Proc Natl Acad Sci USA 96:7370–7375. doi:10.1073/pnas.96.13.7370

10. Kaplan RN, Riba RD, Zacharoulis S, Bramley AH, Vincent L, Costa C, MacDonald DD, Jin DK, Shido K, Kerns SA, Zhu Z, Hicklin D, Wu Y, Port JL, Altorki N, Port ER, Ruggero D, Shmelkov SV, Jensen KK, Rafii S, Lyden D (2005) VEGFR1-positive haematopoietic bone marrow progenitors initiate the pre-metastatic niche. Nature 438:820–827. doi:10.1038/nature04186

11. Kolossov E, Bostani T, Roell W, Breitbach M, Pillekamp F, Nygren JM, Sasse P, Rubenchik O, Fries JW, Wenzel D, Geisen C, Xia Y, Lu Z, Duan Y, Kettenhofen R, Jovinge S, Bloch W, Bohlen H, Welz A, Hescheler J, Jacobsen SE, Fleischmann BK (2006) Engraftment of engineered ES cell-derived cardiomyocytes but not BM cells restores contractile function to the infarcted myocardium. J Exp Med 203:2315–2327. doi:10.1084/jem.20061469

12. Krijnen PA, Hahn NE, Kholova I, Baylan U, Sipkens JA, van Alphen FP, Vonk AB, Simsek S, Meischl C, Schalkwijk CG, van Buul JD, van Hinsberg VW, Niessen HW (2012) Loss of DPP4 activity is related to a prothrombogenic status of endothelial cells: implications for the coronary microvasculature of myocardial infarction patients. Basic Res Cardiol 107:1–13. doi:10.1007/s00395-011-0233-5

13. Lahteenvuo JE, Lahteenvuo MT, Kivela A, Rosenlew C, Falkevall A, Klar J, Heikura T, Rissanen TT, Vahakangas E, Korpisalo P, Enholm B, Carmeliet P, Alitalo K, Eriksson U, Yla-Herttuala S (2009) Vascular endothelial growth factor-B induces myocardium-specific angiogenesis and arteriogenesis via vascular endothelial growth factor receptor-1- and neuropilin

receptor-1-dependent mechanisms. Circulation 119:845–856. doi:10.1161/CIRCULATIONAHA.108.8164

14. Lassaletta AD, Chu LM, Sellke FW (2011) Therapeutic neovascularization for coronary disease: current state and future prospects. Basic Res Cardiol 106:897–909. doi:10.1007/s00395-011-0200-1

15. Li J, Brown LF, Hibberd MG, Grossman JD, Morgan JP, Simons M (1996) VEGF, flk-1, and flt-1 expression in a rat myocardial infarction model of angiogenesis. Am J Physiol 270:H1803–H1811

16. Luttun A, Tjwa M, Moons L, Wu Y, Angelillo-Scherrer A, Liao F, Nagy JA, Hooper A, Priller J, De KB, Compernolle V, Daci E, Bohlen P, Dewerchin M, Herbert JM, Fava R, Matthys P, Carmeliet G, Collen D, Dvorak HF, Hicklin DJ, Carmeliet P (2002) Revascularization of ischemic tissues by PlGF treatment, and inhibition of tumor angiogenesis, arthritis and atherosclerosis by anti-flt1. Nat Med 8:831–840. doi:10.1038/nm731

17. Malan D, Wenzel D, Schmidt A, Geisen C, Raible A, Bolck B, Fleischmann BK, Bloch W (2012) Endothelial beta-1 integrins regulate sprouting and network formation during vascular development. Development 137:993–1002. doi:10.1242/dev.045377

18. Marchetti S, Gimond C, Iljin K, Bourcier C, Alitalo K, Pouyssegur J, Pages G (2002) Endothelial cells genetically selected from differentiating mouse embryonic stem cells incorporate at sites of neovascularization in vivo. J Cell Sci 115:2075–2085

19. Marti HH, Risau W (1998) Systemic hypoxia changes the organ-specific distribution of vascular endothelial growth factor and its receptors. Proc Natl Acad Sci USA 95:15809–15814. doi:10.1073/pnas.95.26.15809

20. Milberg P, Klocke R, Frommeyer G, Quang TH, Dieks K, Stypmann J, Osada N, Kuhlmann M, Fehr M, Milting H, Nikol S, Waltenberger J, Breithardt G, Eckardt L (2011) G-CSF therapy reduces myocardial repolarization reserve in the presence of increased arteriogenesis, angiogenesis and connexin 43 expression in an experimental model of pacing-induced heart failure. Basic Res Cardiol 106:995–1008. doi:10.1007/s00395-011-0230-8

21. Nagy A, Gocza E, Diaz EM, Prideaux VR, Ivanyi E, Markkula M, Rossant J (1990) Embryonic stem cells alone are able to support fetal development in the mouse. Development 110:815–821

22. Neufeld G, Cohen T, Gengrinovitch S, Poltorak Z (1999) Vascular endothelial growth factor (VEGF) and its receptors. FASEB J 13:9–22

23. Oerlemans MI, Goumans MJ, van MB, Clevers H, Doevendans PA, Sluijter JP (2012). Active Wnt signaling in response to cardiac injury. Basic Res Cardiol 105:631–641. doi:10.1007/s00395-010-0100-9

24. Ohtani K, Dimmeler S (2011) Control of cardiovascular differentiation by microRNAs. Basic Res Cardiol 106:5–11. doi:10.1007/s00395-010-0139-7

25. Peters KG, De VC, Williams LT (1993) Vascular endothelial growth factor receptor expression during embryogenesis and tissue repair suggests a role in endothelial differentiation and blood vessel growth. Proc Natl Acad Sci USA 90:8915–8919. doi:10.1073/pnas.90.19.8915

26. Quinn G, Ochiya T, Terada M, Yoshida T (2000) Mouse flt-1 promoter directs endothelial-specific expression in the embryoid body model of embryogenesis. Biochem Biophys Res Commun 276:1089–1099. doi:10.1006/bbrc.2000.3602

27. Redick SD, Bautch VL (1999) Developmental platelet endothelial cell adhesion molecule expression suggests multiple roles for

a vascular adhesion molecule. Am J Pathol 154:1137–1147. doi:10.1016/S0002-9440(10)65366-7

28. Roell W, Lewalter T, Sasse P, Tallini YN, Choi BR, Breitbach M, Doran R, Becher UM, Hwang SM, Bostani T, von MJ, Hofmann A, Reining S, Eiberger B, Gabris B, Pfeifer A, Welz A, Willecke K, Salama G, Schrickel JW, Kotlikoff MI, Fleischmann BK (2007) Engraftment of connexin 43-expressing cells prevents post-infarct arrhythmia. Nature 450:819–824. doi:10.1038/nature06321

29. Roell W, Lu ZJ, Bloch W, Siedner S, Tiemann K, Xia Y, Stoecker E, Fleischmann M, Bohlen H, Stehle R, Kolossov E, Brem G, Addicks K, Pfitzer G, Welz A, Hescheler J, Fleischmann BK (2002) Cellular cardiomyoplasty improves survival after myocardial injury. Circulation 105:2435–2441. doi:10.1161/01.CIR.0000016063.66513.BB

30. Sacchetti A, El ST, Nasr AF, Alberti S (2001) Efficient GFP mutations profoundly affect mRNA transcription and translation rates. FEBS Lett 492:151–155. doi:10.1016/S0014-5793(01)02246-3

31. Stankunas K, Ma GK, Kuhnert FJ, Kuo CJ, Chang CP (2010) VEGF signaling has distinct spatiotemporal roles during heart valve development. Dev Biol 347:325–336

32. Ulyatt C, Walker J, Ponnambalam S (2011) Hypoxia differentially regulates VEGFR1 and VEGFR2 levels and alters intracellular signaling and cell migration in endothelial cells. Biochem Biophys Res Commun 404:774–779

33. Wenzel D, Knies R, Matthey M, Klein AM, Welschoff J, Stolle V, Sasse P, Roll W, Breuer J, Fleischmann BK (2009) Beta(2)-adrenoceptor antagonist ICI 118,551 decreases pulmonary vascular tone in mice via a G(i/o) protein/nitric oxide-coupled pathway. Hypertension 54:157–163. doi:10.1161/HYPERTENSIONAHA.109.130468

34. Wenzel D, Rieck S, Vosen S, Mykhaylyk O, Trueck C, Eberbeck D, Trahms L, Zimmeremann K, Pfeifer A, Fleischmann BK (2012) Identification of magnetic nanoparticles for combined positioning and lentiviral transduction of endothelial cells. Pharm Res. doi:10.1007/s11095-011-0657-5

35. Witmer AN, Dai J, Weich HA, Vrensen GF, Schlingemann RO (2002) Expression of vascular endothelial growth factor receptors 1, 2, and 3 in quiescent endothelia. J Histochem Cytochem 50:767–777. doi:10.1177/002215540205000603

36. Wobus AM, Wallukat G, Hescheler J (1991) Pluripotent mouse embryonic stem cells are able to differentiate into cardiomyocytes expressing chronotropic responses to adrenergic and cholinergic agents and Ca^{2+} channel blockers. Differentiation 48:173–182

37. Wu J, Li J, Zhang N, Zhang C (2011) Stem cell-based therapies in ischemic heart diseases: a focus on aspects of microcirculation and inflammation. Basic Res Cardiol 106:317–324. doi:10.1007/s00395-011-0168-x

38. Xiao J, Moon M, Yan L, Nian M, Zhang Y, Liu C, Lu J, Guan H, Chen M, Jiang D, Jiang H, Liu PP, Li H (2012) Cellular FLICE-inhibitory protein protects against cardiac remodelling after myocardial infarction. Basic Res Cardiol 107:1–21. doi:10.1007/s00395-011-0239-z

39. Zentilin L, Puligadda U, Lionetti V, Zacchigna S, Collesi C, Pattarini L, Ruozi G, Camporesi S, Sinagra G, Pepe M, Recchia FA, Giacca M (2010) Cardiomyocyte VEGFR-1 activation by VEGF-B induces compensatory hypertrophy and preserves cardiac function after myocardial infarction. FASEB J 24:1467–1478